Provided for non-commercial research and education use.
Not for reproduction, distribution or commercial use.

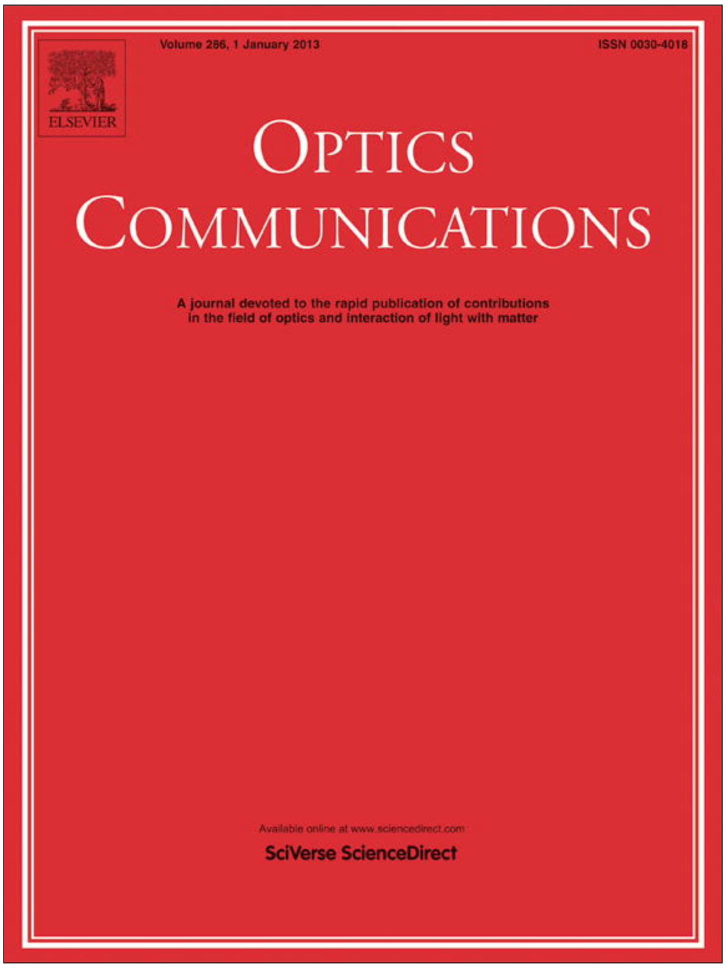

This article appeared in a journal published by Elsevier. The attached copy is furnished to the author for internal non-commercial research and education use, including for instruction at the authors institution and sharing with colleagues.

Other uses, including reproduction and distribution, or selling or licensing copies, or posting to personal, institutional or third party websites are prohibited.

In most cases authors are permitted to post their version of the article (e.g. in Word or Tex form) to their personal website or institutional repository. Authors requiring further information regarding Elsevier's archiving and manuscript policies are encouraged to visit:

http://www.elsevier.com/copyright

Author's personal copy

Optics Communications 286 (2013) 130–134

Contents lists available at SciVerse ScienceDirect

Optics Communications

journal homepage: www.elsevier.com/locate/optcom

Generalization of the Principal Component Analysis algorithm for interferometry

J. Vargas [a,*], C.O.S. Sorzano [a], J.C. Estrada [b], J.M. Carazo [a]

[a] Biocomputing Unit, Centro Nacional de Biotecnología-CSIC, C/ Darwin 3, 28049, Cantoblanco (Madrid), Spain
[b] Centro de Investigaciones en Óptica A. C., Loma del Bosque 115, Col. Lomas del Campestre, 37150, León (Guanajuato), Mexico

ARTICLE INFO

Article history:
Received 6 October 2011
Received in revised form
1 September 2012
Accepted 5 September 2012
Available online 21 September 2012

Keywords:
Phase-Shifting Interferometry
Principal Component Analysis
Least squares minimization

ABSTRACT

This paper presents a generalization of the Principal Component Analysis (PCA) demodulation method. The accuracy of the traditional method is limited by the number of fringes in the interferograms and it cannot be used when there are one or less interferometric fringes. The Advanced Iterative Algorithm (AIA) is robust in this case, but it suffers when the modulation and/or the background illumination maps are spatially dependant. Additionally, this method requires a starting guess. The results and the performance of the algorithm depend on this starting point. In this paper, we present a generalization of the PCA method that relaxes the PCA and AIA limitations combining both methods. We have applied the proposed method to simulated and experimental interferograms obtaining satisfactory results. A complete MATLAB software package is provided.

© 2012 Elsevier B.V. All rights reserved.

1. Introduction

Interferometry is a powerful tool that is used in numerous industrial, research and development applications. These include measuring the quality of a variety of manufactured items such as hard disks, drives and magnetic recording heaps, laser and optics for CD and DVD drives, cameras, laser printers, machined parts and components for fiber-optic systems among others [1]. The primary reason interferometry is so useful is because of its non-contact and non-destructive nature and also because it provides very high accuracy and precision – within the nanometer or even amstrong range —. Phase–Shifting Interferometry (PSI) is the most used interferometry technique in optical metrology for measuring the modulating phase of interferograms [2]. In PSI, a sequence of *N*fringe patterns is obtained and demodulated using different approaches as synchronous or asynchronous phase detection methodologies [2–6]. Typically, these interferograms are acquired with known phase-shifts between successive interferograms so that the acquisition is synchronous [2–4]. This "known" temporal carrier may have some mismatch with respect to the actual carrier and therefore, it will appear as a detuning error in the obtained phase [3–4]. However, there exist synchronous techniques that tolerate some degree of detuning [3].

Another class of phase-shifting algorithms, named *self-calibrating*, allow asynchronous interferogram detection without prior knowledge about the different phase-steps between interferograms [5–6]. All these methods are iterative and require an initial guess to start the minimization process, usually by a least-squares minimization. The main drawback of these techniques is that they require the background illumination or DC term and contrast to be spatially constant. On the other hand, as these methods are based on a minimization process, they require a high computational power and processing time. Additionally, the number of interferograms has to be a high enough to assure the solution convergence toward the global minimum, independently of the starting guess used.

A new kind of phase-shifting demodulation method has been recently proposed [7–8]. This method is based on the use of the Principal Component Analysis (PCA) algorithm to demodulate a phase-shifting interferogram sequence. The algorithm is very fast, approximately two orders of magnitude faster than [6]. It is not iterative and does not require an initial guess of the phase-steps; indeed, this approach does not require obtaining the phase-steps that can be randomly distributed to retrieve the modulating phase. Additionally, it does not need the background illumination and contrast to be spatially constant. This approach requires the following approximations to obtain a trustworthy modulating phase; first, there has to be more than one fringe in the interferograms. Secondly, the temporal average over the interferograms sequence should be a good estimation of the background term. Finally, the different phase-shifts must be well distributed in the $[0, 2\pi]$interval range. Among these requirements, the first one, that will be denoted by us as the number of fringes limitation, is the most problematic as it is a limitation about the kind of interferograms that can be demodulated using this method. The interferograms that come from very flat modulating phases must not be processed using this approach. Additionally, the second and third limitations are common to all kind of temporal demodulation approaches.

In this work, we propose a generalization of the PCA demodulation method that overcomes the called, number of fringes limitation. The

* Corresponding author. Tel.: +34 915206382.
E-mail address: jvargas@cnb.csic.es (J. Vargas).

0030-4018/$ - see front matter © 2012 Elsevier B.V. All rights reserved.
http://dx.doi.org/10.1016/j.optcom.2012.09.017

Author's personal copy

proposed method is based on three steps. First we use the PCA demodulating method to obtain a very fast initial estimation of the modulating phase and to compute a new set of phase-shifting interferograms that are free from DC component and noise. Secondly, we obtain from the computed modulating phase and the new interferogram set, the different phase-steps between interferograms. Finally, we use the previously acquired modulating phase, and phase-steps as an initial guess of a least-squares based minimization approach [6] to obtain an accurate modulating phase. Note that the proposed method is free from the PCA number of fringes limitation. Additionally, as the PCA method will filter out efficiently the DC component and noise it will provide a good initial guess of the modulation term, modulating phase and phase-steps; the proposed method does not require the DC and contrast terms to be spatially constant or the number of interferograms to be high. Typically three or four interferograms will be enough. Finally, observe that often the PCA method provides an accurate phase map so typically only one or two iterations will be necessary to converge to the global minimum so the proposed method is not demanding from a computational point of view.

2. Theoretical foundations

In PSI, an interferogram sequence can be described using the following expression:

$$I_n(x,y) = a(x,y) + b(x,y)\cos[\Phi(x,y) + \delta_n] \tag{1}$$

where $a(x, y)$ is the background illumination or DC component, $b(x, y)$ and $\Phi(x, y)$ are the modulation and phase maps, and δ_n are the phase-steps. Expression (1) can be rewritten as,

$$I_n(x,y) = a(x,y) + b(x,y)(\cos[(x,y)]\cos[\delta_n] - \sin[\delta_n]\sin[\Phi x, y)]) \tag{2}$$

From Expression (2) and grouping terms we obtain,

$$I_n = a + \alpha_n I_c + \beta_n I_s \tag{3}$$

where $\alpha_n = \cos[\delta_n]$, $\beta_n = -\sin[\delta_n]$, $I_c = b\cos[\Phi]$, $I_s = b\sin[\Phi]$ and the spatial dependence has been omitted for the sake of clarity. From a set of interferograms the DC component can be estimated by a temporal average as,

$$a^* = \sum_{n=1}^{N} I_n \cong a \tag{4}$$

where the super-index * denotes that the magnitude is estimated, Expression (3) can be rewritten as:

$$\tilde{I}_n = I_n - a = \alpha_n I_c + \beta I_s \tag{5}$$

From Expression (5), it can be seen that any DC filtered interferogram can always be expressed as a linear combination of two signals. Therefore, a phase-shifted interferogram sequence belongs to a two-dimensional vector subspace.

If there is more than one fringe in the interferograms, we have

$$\langle I_c, I_s \rangle = \sum_{x=1}^{N_x}\sum_{y=1}^{N_y} I_c(x,y) I_s(x,y) \cong 0 \tag{6}$$

where N_x and N_y correspond to the number of pixels in the x and y image axis and $\langle I_c, I_s \rangle$ denotes the inner product between I_c and I_s. In this case I_c and I_s signals are nearly in quadrature and, at the same time, form an quasi-orthogonal interferogram basis. This important result shows that, if Expression (6) is fulfilled, then demodulating and orthogonalizing are equivalent processes. On the other hand, if Expression (6) is not met, still any interferogram of the sequence can be expressed as a linear combination of two orthogonal signals. These orthogonal signals form an interferogram basis but they are not quadrature in general so they do not correspond to the sine and cosine of the modulating phase.

2.1. Principal Component Analysis Method

PCA is a technique from statistics for reducing an image or data set [9]. It involves a mathematical procedure that transforms a number of possibly correlated images into the smallest number of uncorrelated images called the principal components. The principal components are linear combinations of the original variables and are the single best subspace of a given dimension in least-square sense. The different principal components are always orthogonal so they always form an orthogonal basis. In practice, the PCA algorithm is based on three steps. Suppose that we have N images of size $N_x \times N_y$. This image set can be expressed in a matrix form as,

$$\mathbf{X} = [x_1, x_2, \ldots, x_N]^T \tag{7}$$

where x_n is a column vector with size $N_x \times N_y$ whose elements are taken columnwise from the *nth* image. In expression (7), $[\cdot]^T$ denotes the transposing operation and X has N rows and $N_x \times N_y$ Columns. From X we can obtain $\tilde{X}$ that is equals to X without background or DC component, and it is given as,

$$\tilde{X} = [\tilde{x}_1, \tilde{x}_2, \ldots, \tilde{x}_N]^T \tag{8}$$

where $\tilde{x}_n = x_n - a$, and a is the background or DC term that can be obtained as a temporal average of the images as shown in (4). The first step of the PCA algorithm consist in obtaining the covariance matrix C from $\tilde{X}$ as

$$\mathbf{C} = \tilde{X}\tilde{X}^T \tag{9}$$

Note that C corresponds to an inner product matrix and it has the following form:

$$C = \begin{pmatrix} \langle \tilde{x}_1, \tilde{x}_1 \rangle & \langle \tilde{x}_1, \tilde{x}_2 \rangle & \ldots & \langle \tilde{x}_1, \tilde{x}_N \rangle \\ \langle \tilde{x}_2, \tilde{x}_1 \rangle & \langle \tilde{x}_2, \tilde{x}_2 \rangle & \ldots & \langle \tilde{x}_2, \tilde{x}_N \rangle \\ \ldots & \ldots & \ldots & \ldots \\ \langle \tilde{x}_N, \tilde{x}_1 \rangle & \langle \tilde{x}_N, \tilde{x}_2 \rangle & \ldots & \langle \tilde{x}_N, \tilde{x}_N \rangle \end{pmatrix} \tag{10}$$

C matrix corresponds to the projection of each vector x_n with the rest of the vectors. In general these vectors are not orthogonal and, therefore, C is not diagonal and has elements different of zero out of its diagonal. Because C is real and symmetric, always it is possible to find a set of real and nonnegative eigenvalues and its corresponding eigenvectors. From matrix theory the covariance matrix can be diagonalized as,

$$D = ACA^T \tag{11}$$

where A is an orthogonal transformation matrix and D is a diagonal matrix. This diagonalization process is the second step of the PCA method and is performed in a practical point of view by the SVD algorithm. The orthogonal transformation matrix A rotates the original vector set $\tilde{X}$ to a new basis in which the different vectors are orthogonal between them and are given as,

$$Y = A\tilde{X} \tag{12}$$

where

$$Y = [y_1, y_2, \ldots, y_N]^T \tag{13}$$

The inner product matrix of this new vector set is given by,

$$D = \begin{pmatrix} \langle y_1, y_1 \rangle & \langle y_1, y_2 \rangle & \ldots & \langle y_1, y_N \rangle \\ \langle y_2, y_1 \rangle & \langle y_2, y_2 \rangle & \ldots & \langle y_2, y_N \rangle \\ \ldots & \ldots & \ldots & \ldots \\ \langle y_N, y_1 \rangle & \langle y_N, y_2 \rangle & \ldots & \langle y_N, y_N \rangle \end{pmatrix} \tag{14}$$

where D is the diagonal matrix shown in (11) and the vectors y_n are orthogonal and uncorrelated and corresponds to the principal components or eigenvectors of the image set.

Author's personal copy

In our case, where the image set is composed by an interferogram sequence that can be decomposed as shown in Expression (5), we are only concerned about the two first principal components with the largest eigenvalues denoted as y_1 and y_2 [7–8]. These two principal components form an orthogonal basis in which every interferogram can be projected. Note that y_1 and y_2 corresponds to I_c and I_s signals if there are more than one fringe in the interferograms as demonstrated in [8]. In this case, the modulating phase can be obtained from:

$$\Phi^* = \arctan\,(y_2/y_1) \tag{15}$$

2.2. New interferograms set and initial guess for the least-squares minimization

In the general case, although expression (15) cannot be exact, we can still obtain a good estimation of the Modulating phase from it. Additionally, we can use the PCA method to effectively subtract the DC component as well as noise of the interferograms. In order to obtain this new and improved interferogram set, we compute the projection of each interferogram in the orthogonal basis composed by only the first and second principal components, y_1 and y_2 as

$$\begin{aligned}\alpha_n^* &= \langle I_n, y_1 \rangle = \sum_{x=1}^{N_x}\sum_{y=1}^{N_y} y_1(x,y) I_n(x,y)\\ \beta_n^* &= \langle I_n, y_2 \rangle = \sum_{x=1}^{N_x}\sum_{y=1}^{N_y} y_2(x,y) I_n(x,y)\end{aligned} \tag{16}$$

and we reconstruct the denoised and DC free interferograms as

$$\tilde{I}^*{}_n = \alpha_n^* y_1 + \beta_n^* y_2 \tag{17}$$

Additionally, we can obtain the different phase-steps from the previously computed α_n^* and β_n^* obtained in Expression (16) and taking into account Expressions.(2) and (3). Effectively, $\alpha_n = \cos[\delta_n]$ and $\beta_n = -\sin[\delta_n]$ and therefore,

$$\delta_n^* = \arctan\,(-\beta_n^*/\alpha_n^*) \tag{18}$$

Finally, we obtain an estimation of the modulation term as

$$b^* = \sqrt{y_1{}^2 + y_2{}^2} \tag{19}$$

2.3. Least-squares minimization

The previously estimated magnitudes, Φ^*, $\tilde{I}^*{}_n$, δ_n^* and b^* can be refined by a least-squares minimization method [6] using them as the initial guess. Expression (5) can be rewritten in order to show the spatial and temporal dependence of the different terms,

$$\tilde{I}_{in} = \alpha_n (I_c)_i + \beta_n (I_s)_i \tag{20}$$

In Expression (20) the sub-index i denotes spatial dependence and n temporal dependence. Note that $(I_c)_i$ corresponds to a one-dimensional reshape of $I_c(x,y)$. We can write the expression of the least-squares error S_i, accumulated for all the images from Expressions. (17) and (20) as

$$S_i = \sum_{n=1}^{N} (a_i^* + \tilde{I}^*{}_{in} - \tilde{I}_{in})^2 = \sum_{n=1}^{N} (a_i^* + \alpha_n^*(y_1)_i + \beta_n^*(y_2)_i - \tilde{I}_{in})^2 \tag{21}$$

Note, that in Expression (21) we have added the term a^* that takes into account a possible small remaining DC term in the interferograms that only can have spatial dependence. For the known α_n^* and β_n^*, the least-squares criteria requires that,

$$\partial S_i/\partial a_i^* = 0,\ \partial S_i/\partial (y_1)_i = 0,\ \partial S_i/\partial (y_2)_i = 0 \tag{22}$$

Eq. (22) yields

$$X_i = [A]^{-1} B_i \tag{23}$$

where

$$[A] = \begin{bmatrix} N & \sum_{n=1}^{N}\alpha_n^* & \sum_{n=1}^{N}\beta_n^* \\ \sum_{n=1}^{N}\alpha_n^* & \sum_{n=1}^{N}(\alpha_n^*)^2 & \sum_{n=1}^{N}\alpha_n^*\beta_n^* \\ \sum_{n=1}^{N}\beta^*{}_n & \sum_{n=1}^{N}\alpha_n^*\beta_n^* & \sum_{n=1}^{N}(\beta_n^*)^2 \end{bmatrix}^T \quad B_i = \left\{ \sum_{n=1}^{N}\tilde{I}^*{}_{in} \quad \sum_{n=1}^{N}\tilde{I}^*{}_{in}\alpha_n^* \quad \sum_{n=1}^{N}\tilde{I}^*{}_{in}\beta_n^* \right\}^T$$
$$X_i = \alpha_i^* \quad (y_1)_i \quad (y_2)_i\,\} \tag{24}$$

From Expressions. (23)–(24), we can refine y_1, y_2 and Φ^* through Expression (15). Once we have refined these magnitudes, we can use them to improve α_n^*, β_n^*. In this case, we assume that we know y_1 and y_2, and we want to obtain α_n^* and β_n^* through least-squares minimization. In this case, the least-squares error S_n, accumulated for all the pixels corresponds to

$$S_n = \sum_{i=1}^{N_x \times N_y} (a_n^* + \tilde{I}^*{}_{in} - \tilde{I}_{in})^2 = \sum_{i=1}^{N_x \times N_y} (a_n^* + \alpha_n^*(y_1)_i + \beta_n^*(y_2)_i - \tilde{I}_{in})^2 \tag{25}$$

Note, that in Expression (25), we have added the term a^* that takes into account a possible small remaining DC term that has only temporal dependence. For the known y_1 and y_2 the least-squares criterion requires that,

$$\partial S_n/\partial a_n^* = 0,\ \partial S_n/\partial \alpha_n^* = 0,\ \partial S_n/\partial \beta_n^* = 0 \tag{26}$$

Eq. (26) yields,

$$X'_n = [A']^{-1} B'_n \tag{27}$$

where

$$[A'] = \begin{bmatrix} N_x \times N_y & \sum_{i=1}^{N_x \times N_y}(y_1)_i & \sum_{i=1}^{N_x \times N_y}(y_2)_i \\ \sum_{i=1}^{N_x \times N_y}(y_1)_i & \sum_{i=1}^{N_x \times N_y}(y_1 y_1)_i & \sum_{i=1}^{N_x \times N_y}(y_1 y_2)_i \\ \sum_{i=1}^{N_x \times N_y}(y_2)_i & \sum_{i=1}^{N_x \times N_y}(y_1 y_2)_i & \sum_{i=1}^{N_x \times N_y}(y_2)_i^2 \end{bmatrix}$$
$$X'_n = \left\{ a_n^* \quad \alpha_n^* \quad \beta_n^* \right\}^T$$
$$B'_n = \left\{ \sum_{i=1}^{N_x \times N_y}\tilde{I}^*{}_{in} \quad \sum_{i=1}^{N_x \times N_y}\tilde{I}^*{}_{in}(y_1)_i \quad \sum_{i=1}^{N_x \times N_y}\tilde{I}^*{}_{in}(y_2)_i \right\}^T \tag{28}$$

From Expressions (27)–(28) we refine α_n^* and β_n^*, and then the amount of phase-shift can be updated from Expression (18). The presented algorithm repeats iteratively until the phase-shift values converge. The convergence criterion is expressed as

$$\max_n |(\delta_n^{*k} - \delta_n^{*k-1})| < \varepsilon \tag{29}$$

where k represents the number of iteration, and ε is the pre-defined accuracy parameter. Typically a value of 10^{-2} (rad) is sufficient.

3. Simulations

In order to show the performance of the proposed method, we have tested it with two simulations. In the rest of the paper we will use gPCA to refer to the proposed generalization PCA demodulation method. Additionally, we will use AIA and PCA to refer to the Advanced Iterative Algorithm [6] and Principal Component demodulation methods [7].

In the first experiment, we use an interferogram set composed by 25 fringe patterns. The interferograms have a size of 340 × 340 px. The phase-shifts are randomly distributed in the [0, 2π]

Author's personal copy

(rad) range. The noise is additive with a standard normal distribution, and the signal to noise ratio is of 10%. In Fig. 1, we show the first four interferograms of the sequence. As can be seen from Fig. 1, there is less than one fringe in the interferograms so the PCA demodulation method will not obtain accurate results. In Fig. 2 we show a profile along row 170 px of the retrieved phases by the proposed gPCA, PCA, and AIA methods. Additionally we show the profile of the reference phase. As can be seen from Fig. 2, the gPCA and AIA phases are very similar to the reference phase. This is not the case for the PCA retrieved phase. The retrieved root-mean-square (*rms*) and peak to valley (*pv*) errors of the difference between the reference, and the retrieved phases, the number of iterations and the processing times are given in Table 1. As can be seen from Table 1, the gPCA and the AIA have similar accuracy but the proposed method only requires two iterations to convergence. Note that the *rms* of the reference phase is 0.65 (rad) so the perceptual retrieved errors are 7%, 94% and 15% obtained by the gPCA, PCA and AIA methods. The processing times are obtained using a 2.67 GHz laptop and processing with MATLAB. Note that the fast processing time of the PCA method makes this method a perfect preprocessing step.

In the second experiment, we use an interferogram set composed by 20 fringe patterns. The noise is additive with a standard normal distribution, the SNR is of 20% and the phase-shifts are randomly distributed in the [0, 2π] (rad) range. In Fig. 3, we show the first four interferograms of the sequence. As can be seen from Fig. 3, the interferograms are affected by a high spatially varying DC term. In Fig. 4 we show the reference theoretical phase map (a) and the phases obtained by the proposed gPCA (b), the PCA (c) and the AIA (d) methods. As can be seen from Fig. 4, the phase map obtained by the AIA is not accurate and has a large detuning error that can be observed from the grey-level distortion that appears in the recovered wrapped phase. The *rms* and *pv* errors, the processing times and the number of iterations are given in . From Table 2 we can observe that with only one iteration the gPCA method obtains the best accuracy results.

Table 1
Retrieved root-mean-square errors (*rms*), peak to valley (*pv*) errors, number of iterations and processing times obtained in the first simulation by the proposed gPCA, PCA and AIA methods.

	gPCA	PCA	AIA
rms (rad)	0.05	0.60	0.10
pv (rad)	0.34	2.1	0.44
# iterations	2	–	50
Time (s)	4.7	0.35	106

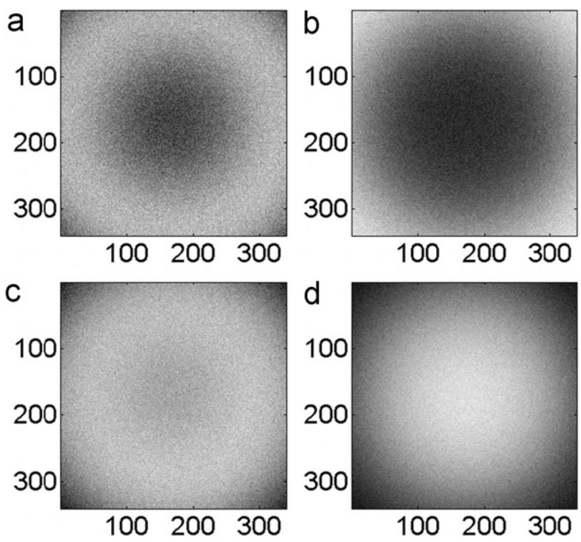

Fig. 1. First four interferograms used in the first simulation.

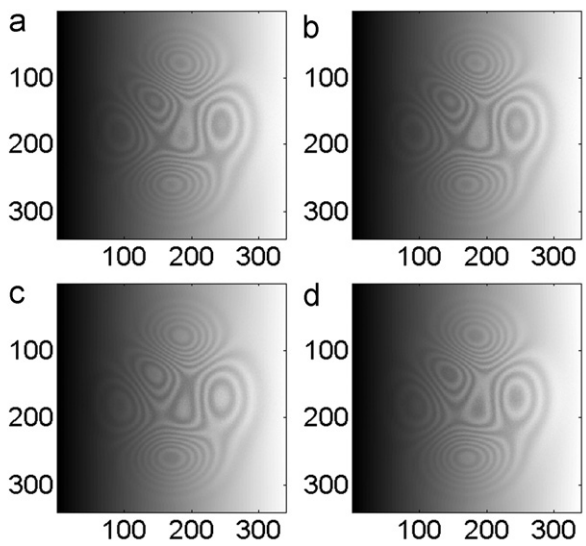

Fig. 3. First four interferograms used in the second simulation.

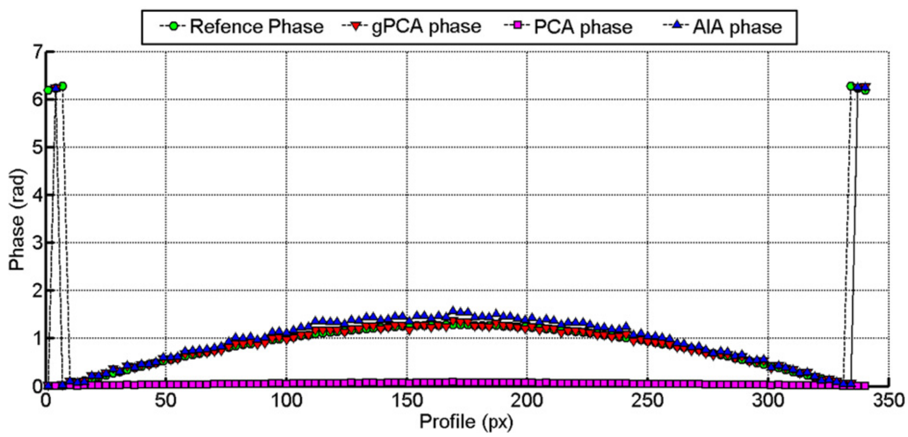

Fig. 2. Profile along row 170 px of the retrieved phases by the proposed Generalized PCA (gPCA), PCA, and AIA methods obtained in the first simulation.

Author's personal copy

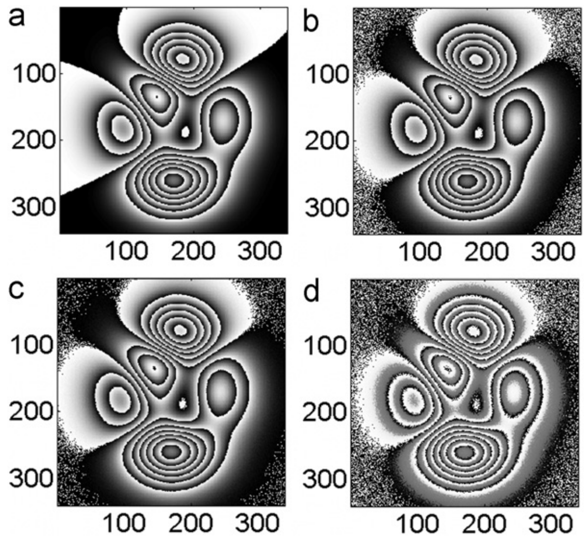

Fig. 4. Reference phase map (a), and wrapped phases by the proposed gPCA (b), PCA (c) and AIA (d) methods obtained in the second simulation.

Table 2
Retrieved root-mean-square errors (*rms*), peak to valley (*pv*) errors, number of iterations and processing times obtained in the second simulation by the proposed gPCA, PCA and AIA methods.

	gPCA	PCA	AIA
rms (rad)	0.073	0.11	0.65
pv (rad)	0.62	0.63	6.2
# iterations	1	–	50
Time (s)	2.5	0.27	95

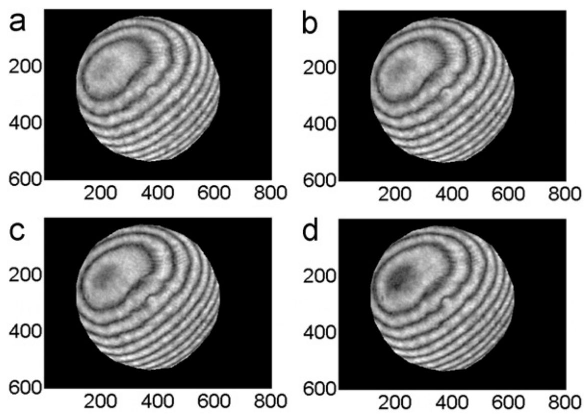

Fig. 5. First four interferograms used in the experimental results section.

4. Experimental results

We have also applied the proposed algorithm to real interferograms. We have compared the retrieved phase from six phase-shifted interferograms using the proposed gPCA, the PCA and the AIA methods. In order to compare the different retrieved phases, we have obtained a reference phase map from a larger interferogram set composed by 20 interferograms and using the PCA method [6]. In Fig. 5 we show the first four used interferograms. Observe from Fig. 5 that we have used a processing mask to subtract the outer region where there are no interferometric fringes. In Fig. 6 we show the reference phase obtained by the PCA algorithm using 20 interferograms (a) and the obtained phases by the proposed gPCA (b), the PCA (c) and the AIA (d) methods using 6 patterns. The *rms* and *pv* errors, the processing times and the number of iterations necessary to converge are presented in Table 3. From Table 3 we can see that in this case, the proposed method has accuracy similar to the rest of approaches and it only requires one iteration.

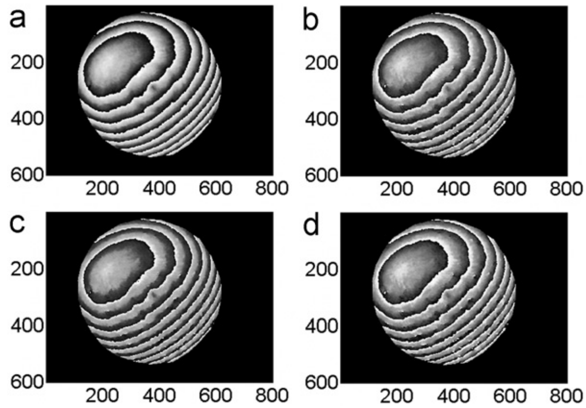

Fig. 6. Reference phase map (a), and wrapped phases by the proposed gPCA (b), PCA (c) and AIA (d) methods obtained using real interferograms.

Table 3
Retrieved root-mean-square errors (rms), peak to valley (pv) errors, number of iterations and processing times obtained in experimental results section by the proposed gPCA, PCA and AIA methods.

	gPCA	PCA	AIA
rms (rad)	0.56	0.57	0.57
pv (rad)	5.8	5.7	5.8
# iterations	1	–	50
Time (s)	3.6	0.15	140

5. Conclusions

We have proposed a generalization of the PCA demodulation method that overcomes the number of fringes limitation of this method. Additionally, the proposed method does not require the DC term and contrast to be spatially constant, high computational power and/or processing time. Additionally, the number of interferograms needs not be high to assure the solution convergence toward the global minimum, independently of the starting point used. So the proposed method is unaffected by the typical limitations of the self-calibrating demodulation methods. The presented approach is based on obtaining a very fast and accurate initial guess of the modulating phase using the PCA demodulation method. Then, this initial estimation is refined through least-squares minimization. We have tested the proposed method with simulated and real interferograms. In all cases, the proposed method presents the highest accuracy when it is compared with the PCA [7] and AIA [6] demodulating methods. All the examples of this work can be reproduced running the MATLAB package that can be found in http://goo.gl/8tQxU.

References

[1] J.C. Wyant, Optics and Photonics News (2003).
[2] D. Malacara, M. Servín, Z. Malacara, Interferogram Analysis for Optical Testing, Marcel Dekker, Inc, 1998.
[3] P. Hariharan, B.F. Oreb, T. Eiju, Applied Optics 26 (13) (1987) 2504.
[4] J.F. Mosino, M. Servin, J.C. Estrada, and J.A. Quiroga, Phasorial analysis of detuning error in temporal phase shifting algorithms, Optics Express 17 (7) (2009) 5618–5623.
[5] I.B. Kong, S.W. Kim, Optics Engineering 34 (1) (1995) 183.
[6] Z.Y. Wang, B.T. Han, Optics Letters 29 (14) (2004) 1671.
[7] J. Vargas, J. Antonio Quiroga, T. Belenguer, Optics Letters 36 (8) (2011) 1326.
[8] J. Vargas, J. Antonio Quiroga, T. Belenguer, Optics Letters 36 (12) (2011) 2215.
[9] R.C. Gonzalez, R.E. Woods, Digital Image Processing, 3rd edition, Prentice Hall, 2008.